Korean J. Chem. Eng., **31**(7), 1194-1203 (2014)
DOI: 10.1007/s11814-014-0052-0

pISSN: 0256-1115
eISSN: 1975-7220

Designing and operating a pilot plant for purification of industrial wastewater from toxic organic compounds by utilizing solar energy

Mohammad Fadhil Abid†, Mohammed Ebrahim, Orroba Nafi, Luma Hussain, Neran Maneual, and Abeer Sameer

Department of Chemical Engineering, University of Technology, Baghdad, Iraq
(*Received 3 September 2013 • accepted 10 February 2014*)

Abstract−The aim of the present project was to design and operate a solar reactor system and to analyze its performance for the removal of different types of toxic organic pollutants (e.g., synthetic methyl violet dye and phenol) from water with titanium dioxide as the photocatalyst. Various operating parameters were studied to investigate the behavior of the designed reactor like initial substrate concentration, loading of catalyst, pH of solution, and H_2O_2 concentration. The operating parameters were optimized to give higher efficiency to the reactor performance. Results showed that a photocatalysis system, operating at optimum conditions, offered within one hour of operation degradation up to 95.27% for synthetic dye, while a conversion of 99.95% was obtained in three hours. With phenol, degradation was up to 80.0% and 98.0%, respectively. The removal of TOC for the two toxic materials was also at high levels. This confirmed the feasibility of the designed solar system. The kinetics of dye degradation was first order with respect to dye concentration and could be well described by Langmuir-Hinshelwood model. A preliminary design of a solar photocatalysis system as an alternative treatment method for wastewater effluents from an Iraqi textile mill was introduced.

Keywords: Solar Photocatalysis, Dye Synthetic Wastewater, Phenol Removal, Degradation Kinetics, Solar Reactor Design

INTRODUCTION

Scientific evidence proves that the effluents released from different industries, such as oil refineries, textile, paints, leather, pesticides, etc., are comprised of different hazardous and toxic compounds, some of which are known to be carcinogens. Also, agricultural activities in the Middle East consume thousands of tons of pesticides annually. Various physical, chemical and biological pre-treatment and post-treatment techniques have been developed over the last two decades to remove organics from contaminated wastewater in order to cost effectively meet environmental regulatory requirements. These treatment techniques currently and commonly practiced for the removal of organic contaminants in industrial wastewaters are inherently problematic in their application. Chemical and biological treatments have been conventionally followed till now, but they have their own disadvantages. The aerobic treatment process is associated with production and disposal of large amounts of biological sludge, while wastewater treated by anaerobic treatment method does not bring down the pollution parameters to a satisfactory level [1]. Chemical treatment methods can prove costly to the user as the active agent cannot be recovered for reuse in successive treatment cycles. Also, the end-product is usually a large amount of sludge requiring final disposal [2]. Air stripping, which is commonly employed for the removal of volatile organic contaminants in wastewater, led to transfer the pollutants from water phase to air phase instead of destroying them. Thus, most air-stripping processes currently require subsequent treatment of the off-gas. Granular activated carbon (GAC) adsorption is the other commercial process for water purification. However, the spent carbon, on which pollutants are adsorbed, is a new waste that requires disposal [3]. Solar energy available in various regions is typically 8.3% ultra-violet (200-400 nm), 38.2% visible (400-700 nm), 28.1% near infra-red (700-1,100 nm) and 25.4% infrared/far-infrared portion [4]. Many researchers have confirmed that it could be possible to degrade a broad range of organics in wastewater by utilizing the solar photocatalysis process [5-7]. Solar photochemical detoxification technology can provide the environmental wastewater management industry with a powerful new tool to destroy wastes with clean energy from the sun. Solar photochemistry technology can be defined as the technology that efficiently collects solar photons and introduces them in an adequate reactor volume to promote specific chemical reactions. Recent laboratory researches [8-11] have proved the reliability of the proposed process, and the availability of sunlight justifies the application of a new detoxification technology. The treatment of contaminated water necessarily includes the design of an efficient photoreactor, which is considered the heart of the process. Iraq and other gulf countries have about 300 days of sunshine per year [12]. So in our research we aimed to design and operate a pilot plant utilizing the solar energy to destroy most of the organic toxic compounds (e.g., synthetic dye, and phenol) present in industrial wastewater. Effects of the operating parameters (i.e., pH of solution, catalyst loading, contaminant concentration, H_2O_2 concentration and liquid flow rate) on reactor performance were investigated.

MATERIALS AND METHODS

1. Materials

Chemicals used in the present work are: hydrogen peroxide (H_2O_2) solution, obtained from Merck was in a stable form (35% (w/w)). To control pH of solution, H_2SO_4 (98%), and NaOH (Flakes) from

†To whom correspondence should be addressed.
E-mail: dr_mfa@uotechnology.edu.iq, doctormfa@gmail.com

Table 1. Equipment of experimental setup

Description	Description	No.
1-Feed tank with stirrer	100 L, PVC	1
2-Discharge tank	100 L, PVC	1
3-Centrifugal pump	PVC lined, Q=2M3, H=36M	1
4-Tubular reactor, pyrex	Φ=30 mm, L=1.5 m, th.=1.5 mm	30
5-U-shape connections	Φ=37 mm, Flex. Rubber	25
6-Valves, elbows	PVC, Φ=25 mm	15, 20, 30 m
7-Aluminum plate	1.5 mm thick. (as designed)	1
8-Flow indicator controller with valve	PVC, F=25 mm	1
9-TOC analyzer	Type (E6811)	1
10-DO-on line monitor	Model 862A	1
11-On-line PH meter	Model excel 25PH/mV/ISL	1

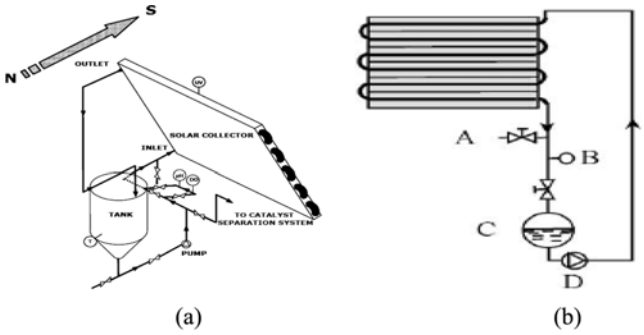

Fig. 1. Schematic diagram of the pilot plant, (a): 3D view and (b): 2D view. A: sampling valve; B: thermocouple; C: feeding tank; D: pump; N: north; S: south.

Fig. 2. A photograhic view of the experimental setup.

Fluke Co. were used. The nanocatalyst (TiO_2, 80% anatasa) of size (5-30 nm) (specific surface area 60±15 m^2/g (BET), was obtained from Zhengzhou Xinyue Chemical Co., China. Synthetic methyl violet 6B ($C_{24}H_{28}N_3Cl$) and analytical grade phenol (C_6H_6O) were supplied from Sigma Aldrich. Other facilities and equipment used for experimental setup and process measurements are shown in Table 1.

2. Methods

2-1. Experimental Setup

All experiments were performed in a photocatalytic reactor with a total volume of 50 L. The photocatalytic reactor was operated as a batch process. The system consists of sunlight collectors, synthetic wastewater preparation tank, circulation pump and a control panel. The solar collector is mounted on a fixed steel platform tilted 37° (local latitude) of the University of Technology-Baghdad with respect to the horizontal plane and facing south. The sunlight collectors were made up of ten Pyrex glass cylindrical tubes 125 cm in length and 3 cm in diameter. The tubes were connected to each other in series by polyethylene cylindrical fittings. A circulating pump was used to feed wastewater from the tank to the solar collectors via a calibrated flow meter and control valve. Aluminum UV-reflective panels were oriented as a parabolic trough shape and placed on the steel structure which was focused on the Pyrex glass tubes. This geometry enables light entering from almost any direction to be reflected into the focal line of the tubes, and the light entering the tubes can also be employed for the photocatalytic reaction. The wastewater preparation tank was made of PVC. The water and reagents were added to the tank from an opening in the lid. A thermocouple was placed at the outlet of the reactor modules to measure the reaction temperature. A mechanical mixer was used to obtain homogeneous conditions in the wastewater tank and to maintain aeration. Two 100 L PVC tanks were used; the first was used for supplying distilled water and the second for collecting the product from the photocatalytic reactor. The whole system was controlled using a control panel. Figs. 1 and 2 represent a schematic drawing and a photographic view of the photocatalytic system, respectively. For further reuse of the catalyst, a low pressure reverse osmosis (LPRO) system was used to separate the catalyst particles from the clean water after the photocatalytic treatment.

2-2. Operating Parameters and Experimental Procedure

Photocatalytic reactor experiments were aimed to study the effect of operating parameters (catalyst loading, hydrogen peroxide concentration, pH and dye or phenol concentration) on the degradation efficiency and TOC removal of organic pollutant. In the present work, factorial design method was used for planning the experiments because of its reliability in finding the effects and interaction between the controlled variables of the operating system [13]. The real values of controlled variables (F) and their corresponding levels (L). The number of experiments needed (N) according to the factorial method is $N=L^F$. 81 experiments were needed for dye study, and the same numbers of experiments were needed for phenol study.

The experimental runs were performed by using the following procedure: first, the prepared aqueous suspension containing the dye or phenol and the TiO_2 powder with H_2O_2 at the desired proportions is circulated from the preparation tank into the reacting system keeping the solar collectors without irradiation by covering them by tarpaulins. The suspension flow rate was maintained constant at all runs at 0.4 L s^{-1}. The Reynolds number value was about 1.8×

10^4 indicating a turbulent flow regime inside the tubes. The total volume (V_T) of the suspension charged in the whole system was 39 L, whereas the irradiated volume (V_i), i.e., the volume of the suspension contained in the glass tubes, was 10.1 L. The dark period continued for 30 min to ensure good distribution of TiO_2 particles in the mixture. When the system was exposed to sunlight, it was recorded as the beginning of illuminated experiment, the reactivity run started. Samples were then withdrawn at the starting of the irradiation at fixed intervals of time (e.g., 30 min) from the preparation tank so that they may represent the conditions at the inlet of the PFR and also from the outlet of the solar modules simultaneously.

2-3. Analytical Methods

Mineralization was followed by measuring the color, which is a function of concentration which was determined at a dominate wavelength by spectrophotometric method no. 2120 Standard Method, using a Shimadzu UV-Visible spectrophotometer (UB-1201 PC). TOC was determined by TOC analyzer type (E6811). To identify the functional groups in the product solutions, FTIR (Bruker Tensor 27) system was used. The sunlight intensity was measured using Davis 6152C Vantage Pro2 Weather Station radiometer. To estimate the concentration of dissolved oxygen, an on-line DO-Model 862A was used. On-line pH meter Model Excel 25PH/mV/ISL was also used to measure the pH of the suspension. Turbidity of water treated by membrane system (LPRO) was measured by Turbid Direct meter (Lovibond). The principle of the spectrophotometer involves light radiation being selectively absorbed when passed through a specific wavelength. An unknown concentration of an organic compound can be determined by measuring the amount of light that a sample absorbs, then applying Beer-Lambert's formula. If the absorbency coefficient is not known, the unknown concentration can be determined using a calibration curve of absorbance versus concentration, constructed from known amounts of a pollutant. The degree of absorption at that specific wavelength is directly proportional to concentration. Thus qualitative and quantitative determination may be made by examining the spectrum and comparison of the absorption with that of a known concentration. Calibration curves of dye and phenol concentrations vs. light absorbance are illustrated in Figs. 3 and 4, respectively.

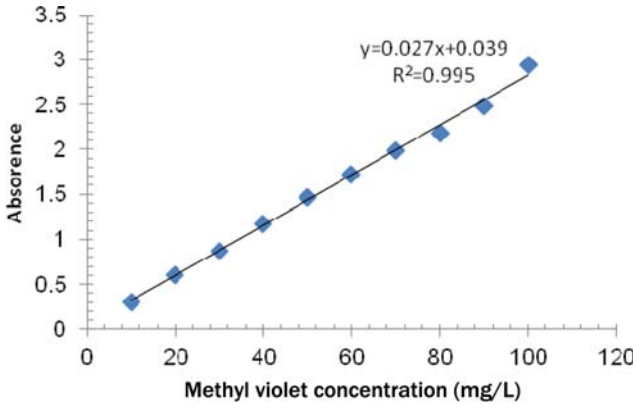

Fig. 3. Calibration curve of light absorbance against methyl violet concentration.

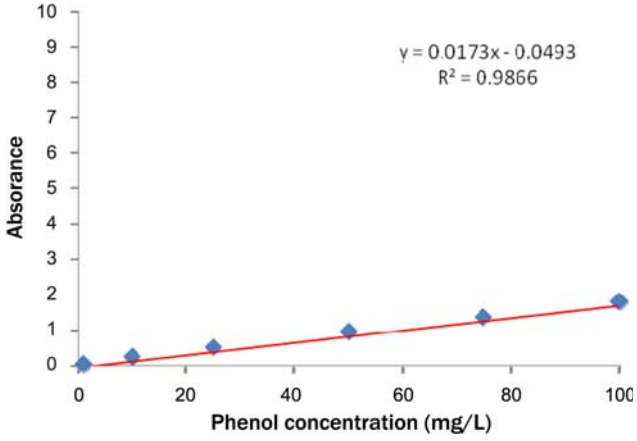

Fig. 4. Calibration curve of light absorbance against phenol concentration.

RESULTS

The reliability of the solar photocatalysis pilot plant was investigated by using different toxic organic compounds. Catalyst concentration, concentration of H_2O_2, pH of solution, and substrate concentration were varied to investigate their effects on the degradation rates and TOC removal of synthetic dye and phenol, respectively. Figs. 5 to 13 illustrate such effects. Results showed that the designed reactor when operating at optimum conditions (i.e., pH=5, $C_{H_2O_2}$=400 mg/L, and C_{TiO_2}=400 mg/L) offered a degradation of MV dye up to 95.27% within one hour of operation time, while a conversion of 99.95% was obtained in three hours. After 180 min of operation, a TOC removal of 99.0% was achieved for MV dye as shown in Figs. 9 to 11. A comparison between mineralization and degradation rates of dye at effluent of reactor. Fig. 13 shows that the initial phenol concentration of 60 mg/L was mineralized from initial TOC equal to 40.62 mg/L to a final TOC of 7.32 mg/L within three hours. This is equivalent to a mineralization efficiency of 81.65%. Effect of accumulated UV energy on degradation rate of different concentrations of MV dye is shown in Fig. 14.

A preliminary design of a solar photocatalysis reactor was conducted as an alternative treatment of a conventional bio-treatment method for Al-Seda textile mill in the governorate of Babylon. Results of preliminary design for the solar system indicated that effective area needed was 25.05 m^2, which is equivalent to 133 Pyrex tubes, each tube of dimensions (27.0 mm ID×2 m Long) to achieve a dye removal of 91.3%. Detailed design procedure is cited in Appendix-A.

DISCUSSION

1. Effect of Operating Parameters on Substrate Degradation in Photocatalytic Reactor

Fig. 5 shows the variation of dye degradation (R %) against illuminated time for various photocatalyst loading by keeping all other parameters unchanged. As can be seen, at a specified catalyst loading the degradation efficiency appeared to increase rapidly at the first part of experimental period, while the rate of increase seems to be slower at the second part. This may be due to the concentration of the dye, which is higher at the beginning of the photodegradation process, resulting in high reaction rate; consequently, as dye

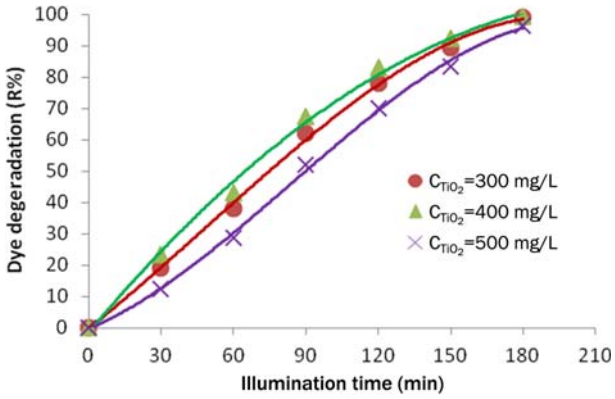

Fig. 5. Variation of dye degradation against time at different concentration of TiO_2 (C_{MV}=30 mg/L, $C_{H_2O_2}$=400 mg/L, pH=5, and Q_L=0.4 L/sec).

concentration decreases the reaction proceeds at a slower rate. Fig. 5 demonstrates a positive impact of catalyst concentration on dye degradation. This trend was almost due to the increase of active sites available for dye adsorption. However, an increase of the catalyst concentration beyond a certain limit would not result in any significant change in the efficiency of degradation. This occurs when the maximum limit of photons absorption is reached within the reactor. From Fig. 5, it was observed that as catalyst concentration increased from (300 to 400 mg/L) the degradation rate increased correspondingly. This can be explained by the fact that there was an increased in the photon adsorption with increasing concentration. The degradation rate decreased as the catalyst loading increased from (400 to 500) mg/L; this phenomenon may be explained by the light scattering, caused by the lightproof suspended catalyst. The results obtained in this work are in agreement with the findings of [14-16].

Fig. 6 plots the variation of dye degradation against H_2O_2 concentration in solution, keeping all other parameters unchanged. Different concentrations of H_2O_2 (400 to 800 mg/L) were added to study the effect of H_2O_2 concentration on the decolorization rate. As can be seen, the removal rate increased with increasing initial concentration of H_2O_2. The decolorization rate was slow at low H_2O_2 concentration, as the formation of hydroxyl radicals was insufficient;

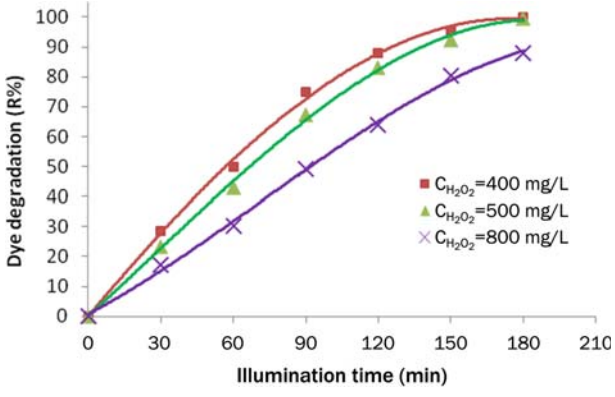

Fig. 6. Variation of dye degradation vs. illuminated time at different concentration of H_2O_2 (C_{MV}=30 mg/L, C_{TiO_2}=400 mg/L, pH=5, and Q_L=0.4 L/sec).

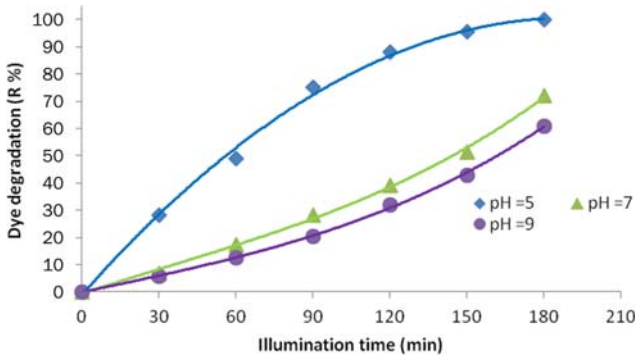

Fig. 7. Variation of dye degradation against illuminated time at different pH (C_{MV}=30 mg/L, C_{TiO_2}=400 mg/L, $C_{H_2O_2}$=400 mg/L, and Q_L=0.4 L/sec).

this may be explained by the ability of H_2O_2 to trap the electrons, preventing the electron-hole recombination and hence increasing the chance of formation of OH* radicals on the surface of the catalyst [17]. However, as the initial concentration of H_2O_2 increased beyond a certain limit, (400 mg/L, the increased decomposition rate became noticeably less. This was because at higher H_2O_2 concentration, more OH* radicals were produced leading to a faster oxidation rate. However, these excess free radicals were more prone to react with the excess H_2O_2 rather than with the dye [16]. One form of this effect can be seen through short-circulating the semiconductor microelectrode [18], according to Eqs. (1) and (2):

$$H_2O_2+\bullet OH \rightarrow H_2O+HO_2 \quad (1)$$

$$HO_2+\bullet OH \rightarrow H_2O+O_2 \quad (2)$$

Therefore, it is imperative to determine the stoichiometric amount of hydrogen peroxide sufficient for complete mineralization. This analysis was not presented in the present work.

Fig. 7 illustrates the variation of dye degradation rate against illuminated time. Results were obtained experimentally by varying initial pH of polluted solution from 5 to 9 with keeping all other parameters unchanged. Fig. 7 clearly indicates a neat decrease in dye degradation with increasing pH values. It can be noticed that the final degradation obtained in acidic solution at pH=5 was 99.95% and at pH=6 it was 95.22%, while at pH=7, and pH=9, the final degradation efficiency was 72.2% and 60.98%, respectively. This could be explained from the surface charge of TiO_2 point of view. In acidic pH, the surface of TiO_2 acquires a positive charge, thereby attracting the anionic MV dye, leading to a greater adsorption and hence increasing the degradation rate in the acidic media. However, the reverse image is observed in the basic medium where the TiO_2 surface was negatively charged, which repels the dye molecules away from the surface of the catalyst, thereby decreasing the degradation rate. The effluent pH affects the surface of titania by protonation or deprotonation according to Eqs. (3) and (4), [19,20].

$$TiOH+H^+ \rightarrow TiOH_2^+ \quad (3)$$

$$TiOH+OH^- \rightarrow TiO^- + H_2O \quad (4)$$

[21] And [20] reported a similar effect of effluent pH on the surface of TiO_2.

The effect of initial concentration of dye solution on dye degra-

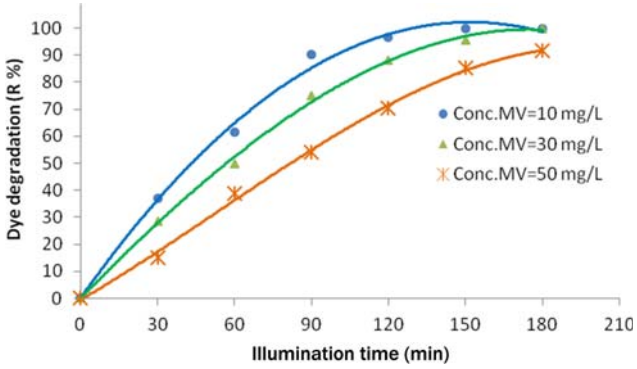

Fig. 8. Variation of dye degradation with illuminated time at different concentration of MV dye ($C_{H_2O_2}$=400 mg/L, C_{TiO_2}=400 mg/L, Q_L=0.4 L/s and pH=5).

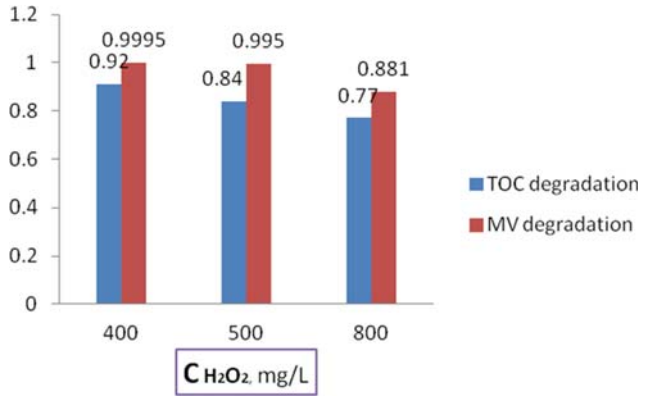

Fig. 10. Effect of H_2O_2 on TOC removal of reactor effluent at (C_{MV}= 30 mg/L, C_{TiO_2}=400 mg/L, pH=5, and Q_L=0.4 L/s).

dation efficiency has been investigated by varying the dye concentrations from (10 to 50 mg/L). Fig. 8 plots the variation of dye degradation against (MV) dye concentration in the presence of 400 mg TiO_2/L under solar light by keeping all other parameters unchanged. As can be seen from Fig. 8 that after 180 min of irradiation time the degradation rate was 99.99%, 99.95%, and 91.52% at MV concentrations of (10, 30, and 50 mg/L), respectively. Dye degradation rate was observed to decrease as initial concentration increased. It could be concluded from the present experiments that as the dye concentration increases, the fraction of the unabsorbed dye in the solution increases, leading to lesser penetration of light through the solution onto the surface of TiO_2, thereby decreasing the rate of formation of OH radicals; consequently the degradation efficiency decreased. However, the reverse image is observed at lower substrate concentration, where the light intensity and time of irradiation are the same, but the interception of the photons by the catalyst surface had increased, leading to the formation of more OH radicals, thereby increasing the rate of reaction. Results obtained in this work are in agreement with the findings of [22].

The initial TOC obtained from adding 30 mg of MV dye to 1,000 ml of distilled water was almost 21.9 mg/L (Figs. 9, 10, and 11). The degradation rate for the mineralization and decomposition of MV at different catalyst loading is shown in Fig. 9. In Fig. 9 a complete MV degradation test is shown and approximately 98% reduction in TOC was observed at the end of 180 min irradiation at optimum operating conditions.

Fig. 9 shows a comparison between dye degradation and mineralization (TOC), which includes the addition of carbon masses of the various intermediate species, as observed with TOC analyzer. Hence, other non-identified intermediate or intermediates are present during MV degradation when using a photocatalyst. The reduction in TOC confirms the mineralization efficiency of the proposed photocatalytic reactor.

Figs. 10 and 11 illustrate the degradation of MV and TOC (mineralization) after 180 min of illumination due to variation in H_2O_2 concentration and pH, respectively, keeping other operating parameters at optimum values. All figures indicate that the degradation of dye concentration is faster than the TOC removal (mineralization).

From these figures, it is interesting that the acidity of solution is a predominant operating parameter in dye degradation and mineralization.

Fig. 12 plots the profiles of removal rates of dye concentration and TOC content, respectively, at optimum operating conditions. As was discussed before, the dye degradation is faster than the mineralization rate. This may be attributed to the formation of organic intermediates as the reaction proceeds, which slows the efficiency of mineralization.

To study the mineralization of phenol, the TOC concentration was monitored against the reaction time and compared with the varia-

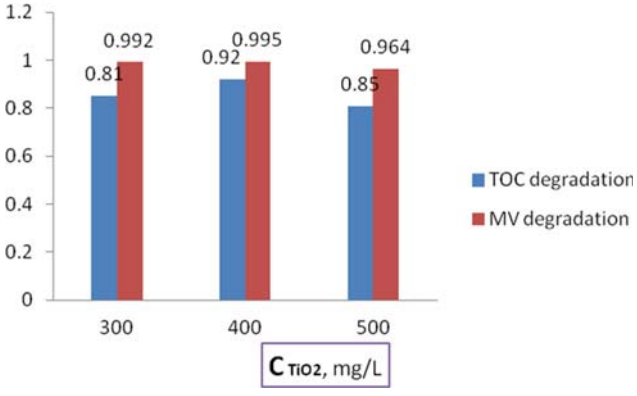

Fig. 9. Effect of catalyst loading on TOC and dye degradation in reactor effluent at (C_{MV}=30 mg/L, TOC=21.9 mg/L, $C_{H_2O_2}$= 500 mg/L, pH=5, and Q_L=0.4 L/s) after 180 min.

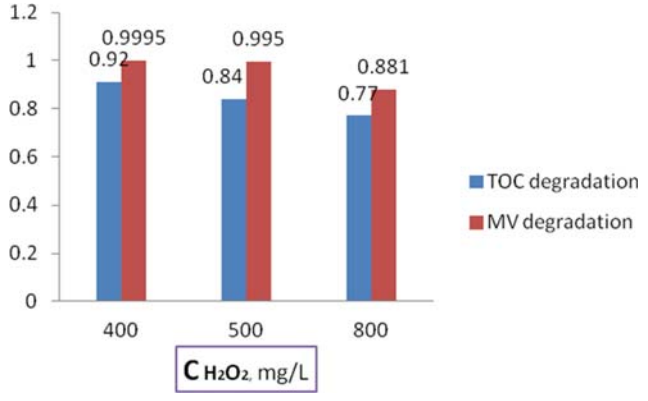

Fig. 11. Effect of pH on TOC removal of reactor effluent at (C_{MV}= 30 mg/L, C_{TiO_2}=400 mg/L, $C_{H_2O_2}$=400 mg/L, and Q_L=0.4 L/s).

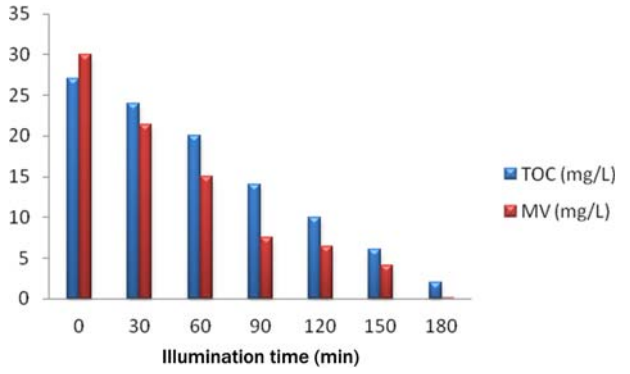

Fig. 12. Variation of mineralization of TOC and removal of dye with illuminated time at ($C_{H_2O_2}$=400 mg/L, C_{TiO_2}=400 mg/L, Q_L=0.4 L/s and pH=5).

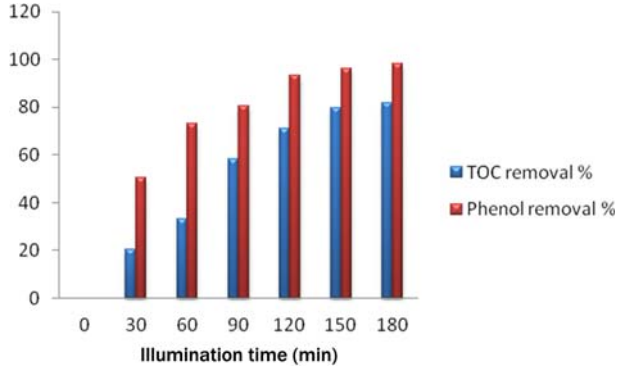

Fig. 13. Variation of mineralization of TOC and removal of phenol with illuminated time at ($C_{H_2O_2}$=400 mg/L, C_{TiO_2}=400 mg/L, Q_L=0.4 L/sec and pH=5).

tion of phenol concentration as shown in Fig. 13. These photocatalytic experiments were conducted under initial phenol concentration of 60 mg/L, pH=5, $C_{H_2O_2}$=400 mg/L, and C_{TiO_2}=400 mg/L. The phenol concentration and TOC concentration were reduced slowly during the reaction period, but the former was reduced faster than the latter. After 3.0 hr reaction time, the phenol removal was 98.1% and the TOC removal was 81.65%, which indicates the reaction has only achieved an incomplete mineralization of phenol, and a longer irradiation time is needed for phenol to complete mineralization.

2. Effect of Accumulated UV Energy on Degradation Rate

In comparison with artificial UV light, the intensity of UV solar energy is time dependent. It is measured by an UV radiometer mounted at the same angle as the solar collector. As radiation data are collected continuously, it is very easy to calculate the global average incident radiation on the collector surface (UV_{avg}, W/m^2). The amount of energy collected by the reactor (per unit volume) from the start of the experiment until each sample is collected may be found by:

$$Q_{UV,n} = Q_{UV,n-1} + \Delta t_n * UV_{avg} * \frac{A}{V}$$

where Δt=time interval between each sample (=30 min), A=area of reactor (=total surface area of glass tubes)=1.175 m^2, V (total volume of the system)=39 L, n=number of samples. The results are shown in Fig. 14, which plots the variation in dye concentration against accumulative UV energy per unit volume of dispersion. The plot depicts that solar energy has a positive impact on the degradation rate of dye, since the oxidation of organics is directly proportional to the concentration of positively charged holes formed by absorption of UV radiation. As can be seen from Fig. 14, the dependence of reaction rate on light intensity (I) undergoes transition from linearity to a non-linear dependence ($I^{0.5}$) as intensity increases. It appears that at high light intensity, the recombination of the electron-hole pair is enhanced, while at low fluxes organic oxidation can compete with recombination. Further, the rate becomes independent of light intensity at higher fluxes and the expected rate-limiting factor becomes the mass transfer. These conclusions are also supported by [23,24].

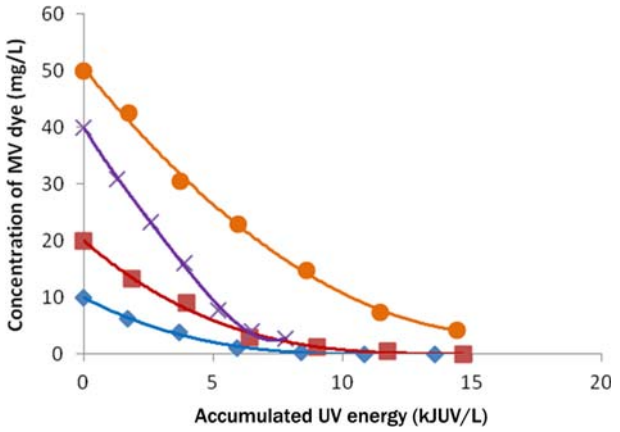

Fig. 14. Variation of concentration of dye vs. Accumulated UV energy with different initial concentration at ($C_{H_2O_2}$=400 mg/L, C_{TiO_2}=400 mg/L, Q_L=0.4 L/s and pH=5).

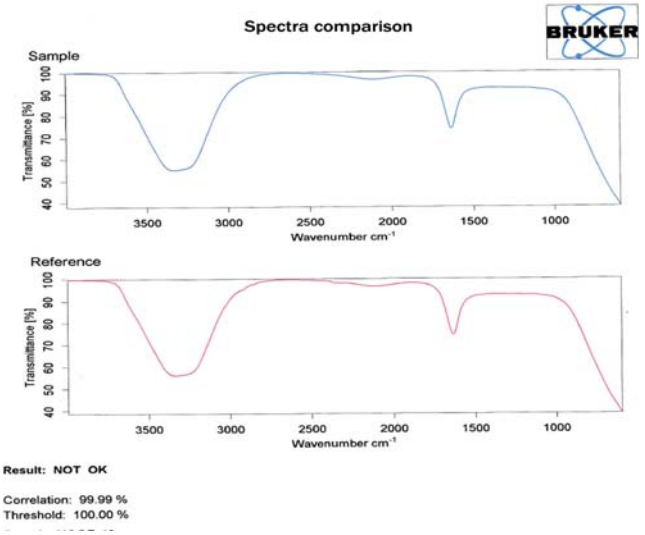

Fig. 15. Contrast of FTIR of MV dye compared with tap water after 180 min under optimum operating conditions.

3. FTIR Measurements

Samples were taken after 180 min from the reactor effluent, after neutralization and filtration with (0.2) μm flat paper, then analyzed with FTIR (type: Bruker Tensor 27). Fig. 15 shows a printout of the FTIR instrument. The figure at the top illustrates the functional groups in the sample taken, while the figure at the bottom shows

an analysis of drinking water. Obviously, the plots confirm that the degradation is almost complete.

4. Catalyst Recuperation

The need to remove the catalyst from the clean water after photocatalytic treatment was initially considered a major disadvantage of a slurry system because efficient separation of the submicron-sized TiO_2 particles from the slurry would be required. Although it is true that titanium dioxide powder particles are about 21 nm, or even smaller in some cases (specially manufactured TiO_2 can be up to 0.01 μm), once in water, the particles always agglomerate into larger ones (from 0.3 to 0.6 μm), facilitating the problem considerably. Recovery rates of over 99% have been obtained and no titanium dioxide has been detected in water filtered with membranes [34]. The lifetime of membranes and the time between cleanings is also increased considerably. This could be particularly important with high volumes of water. Titanium dioxide sedimentation is closely related to colloidal stability and TiO_2 aggregation conditions. The suspension can easily be destabilized by adding an electrolyte (such as NaCl) and/or adjusting the pH to point zero charge (PZC) and the isoelectric point (IEP) on the surface of the catalyst particles, as both factors modify the surface charge. Progressive particle agglomeration (sizes from 1 to 10 μm) and settlement is then obtained. In the case of TiO_2 (Degussa P-25), at concentrations of 400 mgL^{-1}, the PZC is obtained at about pH 7 (6.9±0.2), when NaCl concentration is about 10^{-6} molar. Therefore, more than 200 hours is needed for 75% of titanium dioxide to settle at pH 4.5, but at pH 7, only 4 hours of storage is needed to recover 90 to 95% [25].

In the present work, the pH of the effluent from the photocatalytic reactor was neutralized in a 5 L vessel and then left for four hours. After that the solution was filtered with 0.2 μm flat membrane. The sediment was dried and weighted. The filtrate was fed to the membrane system. Table 2 presents the turbidity before and after the neutralization process measured by turbid direct meter (Lovibond).

5. Photocatalysis Kinetic Study

Photocatalytic destruction of pollutants in aqueous solutions using TiO_2 as nanocatalyst is facilitated mainly by a series of hydroxylation reactions initiated by hydroxyl radicals (˙OH) [26,27]. Possible modes of ˙OH generation during photocatalysis are shown in Fig. 16. Upon UV light illumination, electron-hole pairs are formed in the TiO_2 semiconductor photocatalyst. Holes are positive charges, which when in contact with water molecules, produce ˙OH and H^+ ions. Electrons react with dissolved oxygen to form superoxide ions ($O_2^{\cdot}$), which react with water molecules to produce hydroxide ions (OH^-) and peroxide radicals (˙OOH). Peroxide radicals combine with H^+ ions to form ˙OH and OH^-, and holes oxidize OH^- to ˙OH. Thus, all species eventually facilitate the formation of ˙OH, and these radicals attack the pollutants present in the aqueous solution. TiO_2 powder- is characterized by high stability, good performance and low cost [28].

Table 2. Variation in turbidity against C_{TiO_2} before and after neutralization process

Exp. No.	C_{TiO_2} (mg/L)	Turbidity input (NTU)	Residual turbidity (NTU)
1	300	3300	351.845
2	400	5320	416.405
3	500	5820	459.445

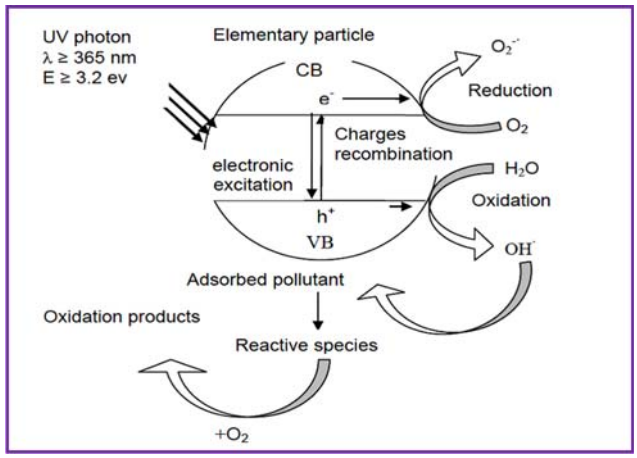

Fig. 16. Principle mechanisms of photocatalysis [27].

The kinetics of the photocatalytic degradation of aqueous pollutants by TiO_2 is still a subject of studies. Several recent reports claim that it follows the Langmuir-Hinshelwood model (L-H model) of kinetics [29]. However, the validity of L-H model in photocatalytic degradation reactions could rather be an easier way of interpretation. Therefore, reporting L-H model of kinetics in photocatalytic degradation without proper experimental evidences is dubious. This model, developed by Turchi et al. [30] and Emeline et al. [31], is expressed as Eq. (5):

$$r=k.\theta=-dC/dt=k.\quad [KC/(1+KC)] \tag{5}$$

where r is the reaction rate ($mg\ L^{-1}min^{-1}$), is the reaction rate constant ($L\ mg^{-1}min^{-1}$), K is the adsorption equilibrium constant of dye (Lmg^{-1}), θ is the fractional site coverage for the reactant, and C is the concentration of dye (mg/L).

The degradation rate of dye was studied as a function of the initial dye concentration in the range (10 to 50 mgL^{-1}), for a catalyst loading of TiO_2 (400 mg/L). The results are illustrated in Fig. 17 which shows the initial dye concentration versus reactor operating time.

Eq. (6) depicts a pseudo-first-order reaction with respect to the methyl violet (MV) concentration. The relationship between the initial degradation rate (r_0) and the initial concentration of organic substrate for a heterogeneous photocatalytic degradation process

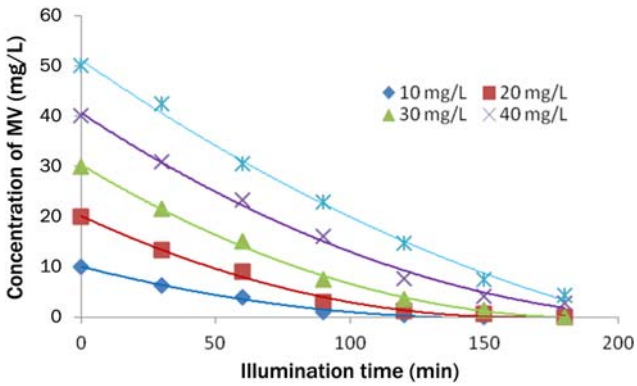

Fig. 17. Effect of initial concentration of MV on the photocatalytic degradation at optimum operating conditions.

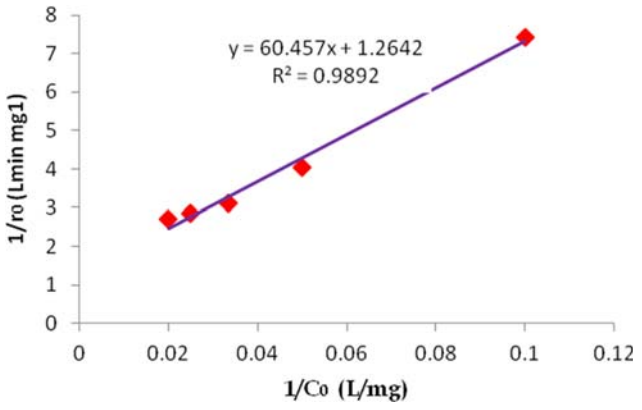

Fig. 18. Linearization of Langmuir-Hinshelwood's equation for MV (C_{TiO_2}=0.4 gL^{-1}, Q=0.5 $Lmin^{-1}$, pH=5, $C_{H_2O_2}$=0.4 gL^{-1}).

has been described by Langmuir-Hinshelwood model and can be written as follows: if we consider that the kinetics of dye degradation is of pseudo-order, at t=0 and C=C_0, Eq. (5) becomes:

$$r_0=k.KC_0/(1+KC_0) \quad (6)$$

This equation can be rearranged into linear form:

$$1/r_0=(1/k.K).1/C_0+1/k_r \quad (7)$$

where $1/r_0$ and $1/C_0$ are the dependent and independent variables, respectively. 1/k is the intercept and (1/k K) is the slope of the straight line shown in Fig. 18. The L-H adsorption constant and the rate constant are obtained using initial rate method [32] by plotting $1/r_0$ versus $1/C_0$. The values of the adsorption equilibrium constant, K and the kinetic rate constant of surface reaction, k, are calculated. The graphical representation of Eq. (7) yields a straight line as shown in Fig. 18, indicating a pseudo-first-order reaction. The reaction rate constants k for photocatalytic degradation of dye are evaluated from experimental data (Fig. 18) using linear regression. The R^2 (correlation coefficient), confirms the proposed kinetics for degradation of phenol in this process. The constants k and K in Langmuir-Hinshelwood model are obtained as 0.791 ($mgL^{-1}min^{-1}$) and 0.0209 Lmg^{-1} for k and K, respectively. The correlation coefficient R^2 is equal to 0.9892; then Eq. (6) will become,

$$r=0.0165\ C/(1+0.0209\ C) \quad (8)$$

Laoufi et al. [27] performed kinetic experiments of degradation of phenol in water solution by TiO_2 photocatalysis in a helical reactor at 32 °C over a range of phenol concentrations from 2.5 to 25 mg l^{-1}, a range of TiO_2 concentrations from 0.1 to 1 g l^{-1}, a range of suspensions pH from 3 to 9. They described the kinetics of phenol by the Langmuir-Hinshelwood (L-H) kinetic model. An overall pseudo-first-order kinetic constant has been calculated for phenol conversion and the values obtained were at 0.1204 mmol. l^{-1} min^{-1} for k and 0.0604 l $mmol^{-1}$ for K, with correlation coefficient R^2 equal to 0.995.

CONCLUSIONS

Results of degradation rate and TOC removal of substrate (i.e., synthetic dye and phenol) by solar photocatalytic reactor indicated the following:

1. It appears that the irradiation time, catalyst load, pH, H_2O_2 concentration, and concentration of substrate mainly control the rate of degradation and TOC removal for which optimum conditions of achieving maximum efficiency were established.

2. At the optimal conditions (i.e., C_{TiO_2}=400 mg/L, $C_{H_2O_2}$=400 mg/L, pH=5) 99.95% and 99% of dye (at concentration=30 mg/L) and phenol (at concentration=25 mg/L) were degraded, respectively after approximately three hours of operation.

3. Regarding catalyst load, the degradation increased with the mass of catalyst up to 400 mg/L. It decreased as the mass continued to increase attributed to the UV light penetration depth, which is considerably smaller than in suspension containing catalyst of 400 mg/L.

4. The capacity of TiO_2 towards substrate degradation strongly depended on the solution pH. At basic pH, degradation was slow, and at acidic pH, degradation of substrate was fast, indicating that the mechanism involving complete mineralization could be achievable under prolonged exposures.

5. The addition of H_2O_2 to TiO_2 suspension resulted in an increase in the degradation rate. The H_2O_2 increased the concentration of $^{\bullet}OH$ radicals and acted as electron acceptors to make electron/hole recombination avoided.

6. It was found that the kinetics of dye degradation was first order with respect to dye concentration and could be well described by Langmuir-Hinshelwood model.

7. The designed setup proved to be efficient for degradation of toxic organic compounds using solar photocatalysis process.

ACKNOWLEDGEMENTS

Authors are thankful to the Department of Chemical Engineering-University of Technology for providing facilities and space where the present work was carried out. The authors gratefully acknowledge the funding of this work by the Arab Science and Technology Foundation (ASTF)- Project no: EN55-. Thanks are also due to the Iraqi Solar Energy Research Center-Baghdad for their assistance. Authors are grateful to Dr. Mohammed Taki Issa Ibrahim for his valuable assistance.

REFERENCES

1. K. Sumandeep, *Light induced oxidative degradation studies of organic dyes and their intermediates*, Ph.D., Thesis, School of Chemistry & Biochemistry Thapar University, PATIALA-INDIA (2007).
2. B. W. Atkinson, F. Bux and H. Kasan, *Water, Air, Soil Pollution*., **24**(2) (1998).
3. D. Chen and A. K. Ray, *Appl. Catal. B: Environ.*, **23**, 143 (1999).
4. S. Chandan, C. Rubina and R. S. Thakur, *Int. J. Energy Environ.* **2**(2), 337 (2011).
5. R. Goslich, R. Dillert and D. Bahnemann, *Water Sci. Technol.*, **35**(4), 137 (1997).
6. S. Ahmed, M. G. Rasul, R. Brown and M. A. Hashib, *J. Environ. Manage.*, **92**(3), 311 (2011).
7. F. Shahrezaei, Y. Mansouri, A. A. L. Zinatizadeh and A. Akhbari, *Int. J. Photoenergy*, **2012**, 1 (2012).
8. D. Robert and S. Malato, *Sci. Total Environ. J.*, **291**, Issue 1-3, 85 (2002).

9. M. Hincapie, M. I. Maldonado, I. Oller, W, Gernjak, J. A. Sanchez-Perez, M. M. Ballesteros and S. Malato, *Solar photocatalytic degradation and detoxification of EU priority substances*, *Environmental Applications of Photocatalysis*, *3rd European Meeting on Solar Chemistry and Photocatalysis: Environmental Applications,* Barcelona, Spain, 203-210, 30 June-2 July (2004).
10. A. García, A. M. Amat, A. Arques, R. Sanchís, W. Gernjak, M. I. Maldonado, I. Oller and S. Malato, *Environ. Chem. Lett.*, **3**(4), 169 (2006).
11. L. Marcos, M. Rosa, I. M. Manuel, M. Sixto and A. P. Jose, *J. Agric. Food Chem*., **57**(23), 11242 (2009).
12. Annual Report of the Iraqi Solar Energy Research Center (ISERC), (2011-2012).
13. A. A. Aldalawi, *Hydrodynamic characteristic effect of foam control in a three-phase bubble column*, MSc Thesis, Chemical Engineering Department, University of Technology, Baghdad, Iraq (2010).
14. N. Guettaï and H. A. Amar, *Desalination*, **185**, 427 (2005).
15. T. Kojima, T. A. Gad-Allah, S. Kato and S. Satokawa, *J. Chem. Eng. Japan*, **44**, 662 (2011).
16. A. Dixit, A. K. Mungray and M. Chakraborty, *Int. J. Chem. Eng. Appl.*, **1**, 247 (2010).
17. Y. Wang and C. S. Hong, *Water Res. J*., **33**, 2031 (1999).
18. U. G. Akpan and B. H. Hameed, *J. Hazard. Mater*., **170**, 520 (2009).
19. I. Poulios and I. Tsachpinis, *J. Chem. Technol. Biotechnol.*, **74**, 349 (1999).
20. M. H. Habibi and H. Vosooghian, *J. Photochem. Photobiol. A: Chem*., **174**, 45 (2005).
21. S. Yang, Y. Chen, J. Zheng and Y. Cui, *J. Environ. Sci*., **19**, 86 (2007).
22. G. Li, T. An, J. Chen, G. Sheng, J. Fu, F. Chen, S. Zhang and H. Zhao, *J. Hazard. Mater*., **138**, 392 (2006).
23. C. A. Parsons, M. W. Peterson, B. R. Thacker, J. A. Turner and A. J. Nozik, *J. Phys. Chem*., **94**, 3381 (1990).
24. M. Kaneko and I. Okura (Eds.), *Photocatalysis: Science and technology*, Springer, Tokyo (2002).
25. B. G. Julian and M. R. Sixto, *Solar detoxification*, United Nations Educational, Scientific and Cultural Organization (2003).
26. C.-S. Lu, C.-C. Chen, F.-D. Mai and H.-K. Li, *J. Hazard. Mater.*, **165**, 306 (2009).
27. N. A. Laoufi, D. Tassalit and F. Bentahar, *Global NEST J.*, **10**(3), 404 (2008).
28. A. Fujishima and X. Zhang, *ComptesRendusChimie*, **9**, 750 (2006).
29. Y. Lin, C. Ferronato, N. Deng, F. Wu and J.-M. Chovelon, *Appl. Catal. B*, **88**, 32 (2009).
30. C. S. Turchi and D. F. Ollis D.F., *J. Catal.*, **122**, 178 (1990).
31. A. V. Emeline, V. Ryabchuk and N. Serpone, *J. Photochem. Photobiol. A: Chemistry*, **133**, 89 (2000).
32. K. H. Wang, Y. H. Hisieh, C. H. Wu and C. Y. Chang, *Chemosphere*, **40**, 389 (2000).
33. S. Malato, J. Blanco, A. R. Fernandez and A. A. Aguera, *J. Chemosphere*, **40**, 403 (2000).
34. K. Okamoto, Y. Yamamoto, H. Tanaka, M. Tanaka, A. Itaya, *Chem. Soc. Jpn*., **58**, 2015 (1985).

APPENDIX A: PRELIMINARY DESIGN EXAMPLE

The example considered is the treatment of water contaminated by synthetic dye (i.e., Methyl violet dye) from the effluent of Al-Seda textile mill at Babylon state. The wastewater discharged from the textile mill has a yearly flow rate of 4,000 m^3 and a dye concentration of 40 mg/L which is then sent to a biological treatment with a basin of dimensions (20×30×2 meter) before being released to the Tigris River at a dye concentration of 4.08 mg/L.

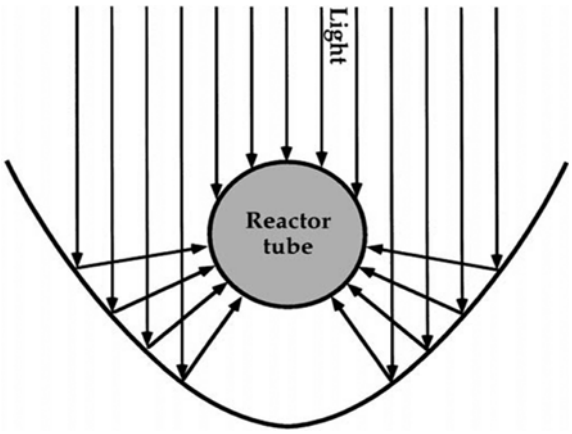

Fig. 1-A. Configuration setup of a parabolic trough collector (PTC).

It is proposed to design a solar photocatalysis plant to degrade the contaminants instead of conventional bio-treatment to match the environmental standards before being released to the river. The main item in the preliminary design is the calculation of the solar collector field surface necessary, for which the following data have either been previously collected or assumed:

- The total volume of wastewater to be treated yearly is 4,000 m^3 (C_{MV}=40 mg/L, which is equivalent to a TOC=29.2 mg/L).
- This would mean a total dye weight of 160 kg (4,000,000 L ×40 mg/L) to be treated yearly by the solar detoxification facility.
- The parabolic trough collector (PTC) type (shown in Fig. 1-A) has been chosen for solar detoxification loops of the plant.

And the following hypotheses have previously been formulated:

- The degradation efficiency of the solar detoxification facility is more than 90%.

The size of the solar field can be calculated with the following design parameters:

- Solar photocatalysis with TiO_2 nanoparticles is the photochemical degradation process selected.
- The initial TOC of water entering the solar detoxification facility will be 29.2 mg/L, which includes not only the active ingredient, but also the rest of the components in the commercial formulation.
- The final TOC signifying water removal from the solar plant is 4.08 mg/L.
- The plant is designed to treat 160 kg of synthetic dye within wastewater discharged from the textile mill process yearly.
- The total volume of water to be treated yearly is 4,000 m^3 (4,000,000 L).
- 3,000 hours of operation yearly.
- The average local global UV irradiation (measured by Davis 6152C Vantage Pro2 Weather Station radiometer) is 30.4 W/m^2.
- The average solar energy necessary to degrade the contaminants is 6.5 kJUV L^{-1} which was calculated using the following equation [33]:

$$Q_{UV,n} = Q_{UV,n-1} + \Delta t_n \times UV_{gN} \times \frac{A}{Vtot} \quad (1)$$

where Δt=time interval between each sample (=30 min), A=effective area of reactor=(π×OD×L×10)=1.18 m^2, V=50 L, n=number of samples to reach the desired degradation.

From Fig. (14), for a degradation=91%, $Q_{UV,n}$=6.5 kJUV/L,

So, using the following equation [25], the collector field area will be:

$$S = \frac{QUV * Vtot}{Hs * UVG} = \frac{6.5 * 10000 * 4000000}{3000 * 3600 * 30.4} = 20.04 \text{ m}^2 \quad (2)$$

And the proposed size of the solar collector field would be 25.05 m^2 (including a 25 percent margin). This is equivalent to 133 Pyrex tubes, each tube of dimensions (30.0 mm OD×2 m Long).